

Electronic Supporting Information

Self-regenerative adsorbent based on the cross-linking chitosan for adsorbing and mineralizing azo dye

Fei Yu^{a, b §}, Lu Chen^{a, c §}, Jie Ma^{a*}, Yiran Sun^a, Qiang Li^a, Chenlu Li^a, Mingxuan Yang^a,
Junhong Chen^{d*}

^a*State Key Laboratory of Pollution Control and Resource Reuse, School of Environmental Science and Engineering, Tongji University, 1239 Siping Road, Shanghai 200092, China*

^b *School of Chemical and Environmental Engineering, Shanghai Institute of Technology, 100 Hai Quan Road, Shanghai 201418, China*

^c *Department of Civil and Environmental Engineering, University of Michigan, 2350 Hayward Street, Ann Arbor, USA*

^d**Department of Mechanical Engineering, University of Wisconsin–Milwaukee, Milwaukee, WI 53211, USA.*

Characterization methods

The microstructure and morphology of the SRCS were analyzed by scanning electron microscopy (SEM, JSM-6400F). X-ray diffraction (XRD) experiments were conducted on specimens using an X-ray diffractometer (Bruker D8 Advance, Bruker AXS, Germany) operating at 40 KV and 40 mA. Nickel-filtered Cu $\text{K}\alpha$ radiation was used in the incident beam. TA Instruments[®] Q600 SDT thermal analyzer was used for high resolution thermogravimetric analysis (TGA) and differential thermal analysis (DTA). TGA and DTA curves were obtained by heating approximately 10 mg of finely powdered samples from 50 to 900°C at a heating rate of 10°C/min in air. X-Ray photoelectron spectroscopy (XPS) analysis was carried out in a Kratos Axis Ultra DLD spectrometer, using monochromated Al Ka X-rays at a base pressure of 1×10^{-9} Torr. Survey scans determined between 1100 and 0 eV revealed the overall elemental compositions of the sample, and regional scans for specific elements were performed. The peak energies were calibrated by placing the major C_{1s} peak at 284.6 eV.

Batch adsorption experiments

The MO concentration was determined colorimetrically by measuring solutions at its maximum absorbance ($\lambda_{\text{max}}=463$ nm). A calibration curve relating the absorbance and concentration of the dye was plotted to obtain the absorbance-concentration profile of the dye based on the Beer-Lambert law¹. Samples of highly concentrated solutions of the dye were diluted before absorbance measurements. Batch adsorption experiments were conducted in 50 mL glass bottles with 30 mg SRCS and 40 mL of MO solution at different initial concentrations of 100~1000 mg/L, and the pH of the

solutions was adjusted to ~7.0 (nearly neutral to avoid unpredictable influences) with HCl or NaOH solutions. Timing of the sorption period started as soon as the solution was poured into the bottle. Sample bottles were shaken on a shaker (TS-2102C, Shanghai Tensuclab Instruments Manufacturing Co., Ltd., China) and maintained at a constant temperature of 25°C and 150 rpm. Preliminary experiments indicated that the adsorption of MO reached equilibrium in ~48 h. Thus, a contact time of 50 h was selected for the batch experiments. All adsorption experiments were conducted in duplicate, and only mean values have been reported. The maximum deviation for the duplicates was usually less than 5%. Blank experiments without the addition of SRCS were conducted to ensure that the decreases in concentration were actually due to adsorption by SRCS, rather than adsorption on the glass bottle wall. After adsorption equilibrium was achieved, the MO concentrations of the solutions were measured using a spectrophotometer (UV759UV-VIS, Shanghai Precision & Scientific Instrument Co. Ltd.). Kinetic studies were performed at a constant temperature of 25°C and 150 rpm with 800 mg/L initial concentration of MO solutions. The effect of solution pH on MO dye removal was studied in the range of 4-10 with the initial concentration of the MO dye solutions set at 600 mg/L. The initial pH values of all the solutions were adjusted using 0.1 mol L⁻¹ HCl or 0.1 mol L⁻¹ NaOH solution.

The amount of adsorbed MO on the adsorbents (q_t , mg/g) was calculated as follows:

$$q_t = (C_0 - C_t) \times \frac{V}{m} \quad (1)$$

where c_0 and c_t are the MO dye concentrations at the beginning and after a period of time t (mg/L), V is the initial solution volume (L), and m is the adsorbent weight (g).

Data analysis

Isotherm model

The form of the Langmuir isotherm can be represented by the following equation:

$$q_e = q_m \frac{K_L C}{1 + K_L C} \quad (2)$$

where q_e is the amount of dye adsorbed per gram of adsorbent (mg/g), C denotes the equilibrium concentration of dye in solution (mg/L); K_L represents the Langmuir constant (L/mg) that relates to the affinity of binding sites and q_m is a theoretical limit of adsorption capacity when the monolayer surface is fully covered with dye molecules to assist in the comparison of adsorption performance (mg/g). Furthermore, the effect of the isotherm shape was studied to understand whether an adsorption system is favorable or not. Another important parameter, R_L , called the separation factor or equilibrium parameter, which can be used to determine the feasibility of adsorption in a given concentration range over adsorbent, was also evaluated from the relation²:

$$R_L = \frac{1}{1 + K_L C_0} \quad (3)$$

where K_L is the Langmuir adsorption constant (l/mg) and C_0 is the initial dye concentration (20mg/l). Ho and McKay³ established that (1) $0 < R_L < 1$ for favorable

adsorption; (2) $R_L > 1$ for unfavorable adsorption; (3) $R_L = 1$ for linear adsorption; and (4) $R_L = 0$ for irreversible adsorption.

Freundlich model

The Freundlich isotherm model has the following form:

$$q_e = K_F C^{1/n} \quad (4)$$

where q_e is the amount of dye adsorbed per gram of adsorbent (mg/g); C is the equilibrium dye concentration in solution (mg/L); K_F and n are the Freundlich constants, which represent the adsorption capacity and the adsorption strength, respectively. The magnitude of $1/n$ quantifies the favorability of adsorption and the degree of heterogeneity of the adsorbent surface.

Dubinin-Radushkevich (D-R) model

The D-R isotherm model has the following form:

$$\ln q_e = \ln q_m - B \varepsilon^2 \quad (5)$$

B , a constant related to the mean free energy of adsorption (mol^2/kJ^2); q_m , the theoretical saturation capacity; and ε , the Polanyi potential, which is equal to

$$\varepsilon = RT \ln\left(1 + \frac{1}{C}\right) \quad (6)$$

where R ($\text{J} \cdot \text{mol}^{-1} \cdot \text{K}^{-1}$) is the gas constant and T (K) is the absolute temperature. For D-R isotherm model, from B values the mean energy of adsorption. E can be calculated using the relation⁴

$$E = \frac{1}{\sqrt{-2B}} \quad (7)$$

Based on equations (5), (6) and (7), the isotherm constants, E and determination coefficients were calculated. The mean energy of adsorption (E) is the free energy change when one mole of the ion is transferred from infinity in the solution to the surface of the solid.

Kinetic model

Pseudo-first and pseudo-second model

The linear form of pseudo first-order rate equation is

$$\ln(q_e - q_t) = \ln q_e - \frac{K_1}{2.303} t \quad (8)$$

where q_e and q_t are the amounts of MO adsorbed (mg/g) at equilibrium and time t (min), respectively; K_1 is the rate constant of the pseudo first-order kinetic model (min^{-1})³.

A linear form of pseudo second-order kinetic model is express by eq. (9)

$$\frac{t}{q} = \frac{1}{k_2 q_e^2} + \frac{t}{q_e} \quad (9)$$

where k_2 is the rate constant($\text{g}\cdot\text{mg}^{-1}\cdot\text{min}^{-1}$) of pseudo second-order kinetic model for adsorption³.

Weber-Morris kinetics model

Intra-particle mass transfer diffusion model proposed by Weber and Morris can be written as follows⁵:

$$q_t = k_i t^{1/2} + C \quad (10)$$

where C (mg/g) is the intercept and k_i is the intra-particle diffusion rate constant ($\text{g}\cdot\text{mg}^{-1}\cdot\text{min}^{-0.5}$) for adsorption.

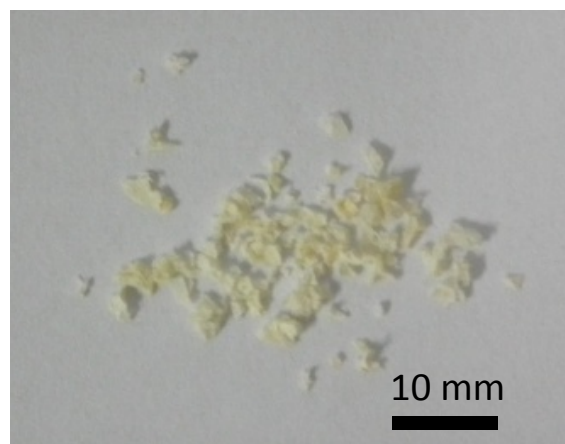


Fig. S1 Optical image of SRCS particles.

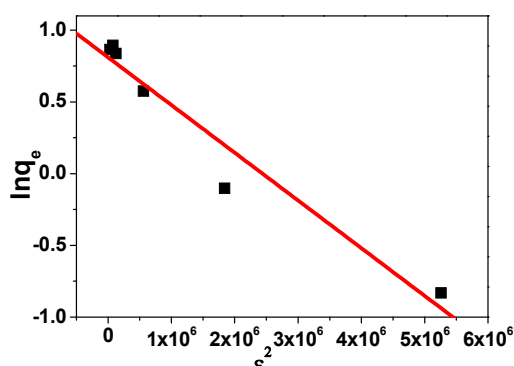


Fig.S2 Dubinin-Radushkevich model on SRCS for MO

To deepen our understanding of the adsorption mechanism, the Dubinin-Radushkevich (D-R) isotherm model was chosen to describe adsorption on both homogenous and heterogeneous surfaces⁶. The D-R model was also applied to distinguish between physical and chemical adsorption of the MO dye on SRCS, as shown in Fig. S2. The isotherm constants, E and R^2 , were calculated and are presented in Table S1. The values of E are $1290 \text{ kJ}\cdot\text{mol}^{-1}$ for the entire range of investigated MO dye concentrations, which suggests that chemical adsorption is dominating in the adsorption process between the MO dye and SRCS adsorbent⁷.

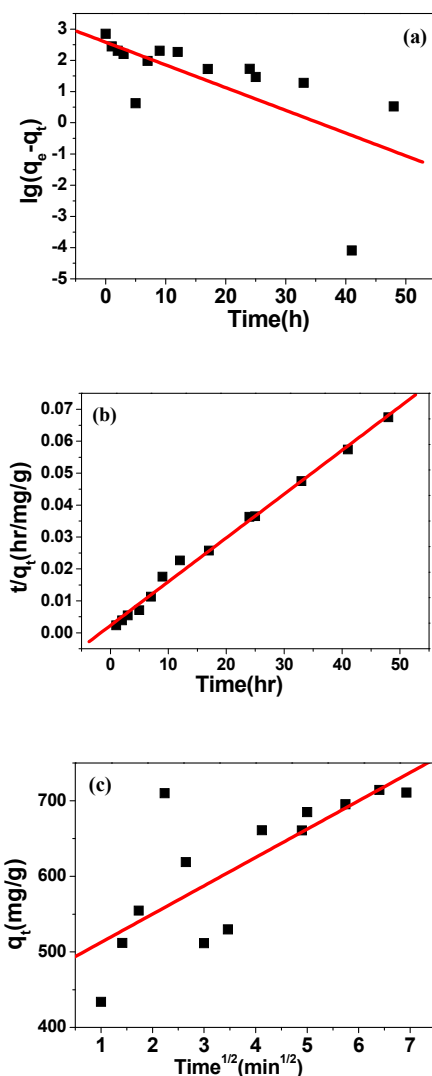


Fig. S3 Pseudo-first-order model (a) , pseudo second-order model (b), and
Weber-Morris model (c) of MO on SRCS.

In order to understand the characteristics of the adsorption process, the pseudo-first-order (PFO) and pseudo-second-order (PSO) kinetic models were applied to fit the experimental data obtained from batch experiments. The kinetic parameters and the determination coefficients were determined by nonlinear regression and are given in Table S2. The R^2 values (~0.96) of the PSO kinetic model are much higher than those of the PFO model, as shown Fig. S2a. The calculated q_e values ($q_{e,cal}$) of

the PSO model are close to the experimental ones ($q_{e,exp}$). Hence, the PSO kinetic model is more appropriate for describing the adsorption behavior of MO onto SRCS, as shown in Fig. S3b.

In order to determine the actual rate-controlling step involved in the MO sorption process, the Weber-Morris equation was applied. Plots of q_t against $t^{1/2}$ are shown in Fig. S2c, and the corresponding kinetic parameters are listed in Table S2. It was also observed that the regression of q_t versus $t^{1/2}$ was non-linear and the plots do not pass through the origin, suggesting that intra-particle diffusion is not the rate-controlling step⁸ and that external mass transfer may also contribute significantly in the rate-controlling step due to the large intercepts of the linear portions of the plots⁹, which also illustrated that there were many macropores on the SRCS surface. So the overall adsorption process may be jointly controlled by external mass transfer and intra-particle diffusion.

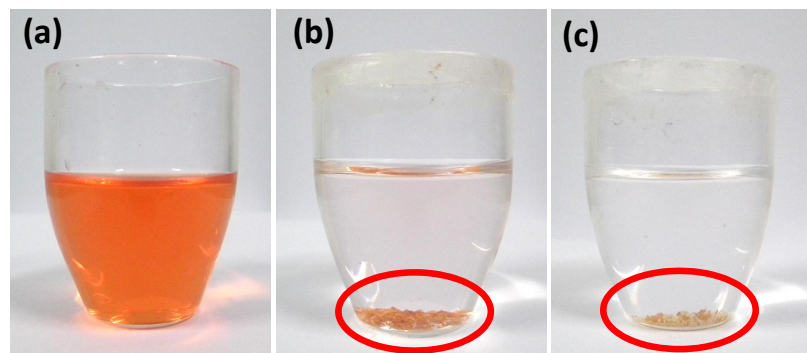


Fig. S4 Optic photos of adsorption and photocatalytic regeneration, (a) before adsorption,(b) after adsorption, (c) after photocatalytic regeneration

Table S1. Langmuir, Freundlich and Dubinin-Radushkevich isotherms parameters of MO adsorption on SRCS

Adsorbent	Adsorbate	Langmuir model			Freundlich model			Dubinin-Radushkevich model			
		$K_L(l/mg)$	$q_m(mg/g)$	R^2	K_F	$1/n$	R^2	$B(mol^2/kJ^2)$	$Q_m(mg/g)$	$E(kJ/mol)$	R^2
SRCS	MO	0.363	799.2	0.941	319.5	0.159	0.721	0.0000003	736.4	1290	0.949

Table S2 Kinetic parameters of pseudo first- and second-order adsorption kinetic models and Weber-Morris model for MO on SRCS. (MO concentration=800 mg/L, SRCS=0.75g/L)

Dye	$q_{e,exp}$	Pseudo first-order model			Pseudo second-order model			Weber-Morris model			
		(mg/g)	$k_1(\text{min}^{-1})$	$q_{e,cal}$	R^2	$k_2(\text{g}\cdot\text{mg}^{-1}\cdot\text{min}^{-1})$	$q_{e,cal}$	R^2	$K_i(\text{g}\cdot\text{mg}^{-1}\cdot\text{min}^{-0.5})$	C	R^2
			(mg/g)				(mg/g)				(mg/g)
MO	714.3	0.077	9.85	0.091	0.003	625	0.962	41.48	464.7	0.237	

Table S3 Chemical composition of SRCS, SRCS-MO, SRCS-R

Sample	O (Atomic%)	Ti (Atomic%)	N (Atomic%)	C (Atomic%)	S (Atomic%)
SRCS	31.53	1.26	5.73	61.48	-
SRCS-MO	30.77	2.10	6.77	59.39	0.97
SRCS-R	31.80	2.75	4.49	60.68	0.28

Reference

1. M. A. Behnajady, N. Modirshahla and H. Fathi, *J Hazard Mater*, 2006, **136**, 816-821.
2. G. H. Sonawane and V. S. Shrivastava, *Desalin Water Treat*, 2011, **29**, 29-38.
3. Y. S. Ho and G. McKay, *Chem Eng J*, 1998, **70**, 115-124.
4. J. P. Hobson, *J. Phys. Chem.*, 1969, **73**, 2720–2727.
5. W. J. Weber and J. C. Morris, *Journal of the Sanitary Engineering Division*, 1963, **89**, 31-60.
6. B. M. Jovanovic, V. L. Vukasinovic-Pesic and L. V. Rajakovic, *Water Environ. Res.*, 2011, **83**, 498-506.
7. S. S. Tahir and N. Rauf, *Chemosphere*, 2006, **63**, 1842-1848.
8. M. Dogan, H. Abak and M. Alkan, *J. Hazard. Mater.*, 2009, **164**, 172-181.
9. Y. S. Al-Degs, M. I. El-Barghouthi, A. A. Issa, M. A. Khraisheh and G. M. Walker, *Water Res.*, 2006, **40**, 2645-2658.